Up to N^{3}LO heavy-baryon chiral perturbation theory calculation for the $M1$ properties of three-nucleon systems

Young-Ho Song[*]
Department of Physics, Duke University, Durham, North Carolina 27708, USA

Rimantas Lazauskas[†]
IPHC, IN2P3-CNRS/Université Louis Pasteur BP 28, F-67037 Strasbourg Cedex 2, France

Tae-Sun Park[‡]
Department of Physics and BAERI, Sungkyunkwan University, Suwon 440-746, Korea
(Received 22 December 2008; published 22 June 2009)

$M1$ properties, comprising magnetic moments and radiative capture of thermal neutron observables, are studied in two- and three-nucleon systems. We use meson exchange current derived up to N^{3}LO using heavy baryon chiral perturbation theory à la Weinberg. Calculations have been performed for several qualitatively different realistic nuclear Hamiltonians, which permits us to analyze model dependence of our results. Our results are found to be strongly correlated with the effective range parameters such as binding energies and the scattering lengths. Taking into account such correlations, the results are in good agreement with the experimental data with small model dependence.

DOI: 10.1103/PhysRevC.79.064002 PACS number(s): 21.45.−v, 11.80.Jy, 25.40.−h, 25.10.+s

I. INTRODUCTION

$M1$ properties—nuclear magnetic moments as well as radiative capture cross sections—are the fundamental low-energy observables of a few nucleon systems and therefore are ideal to test effective field theories (EFTs). In this regard, $M1$ properties have been extensively studied using EFT with huge successes [1–7]. One such example is the ability to describe σ_{np}, the capture cross section of the $np \to d\gamma$ process, at threshold with 1% accuracy by applying heavy-baryon chiral perturbation theory (HBChPT) up to next-next-next-to-leading order or N^{3}LO [1]. In this work, we extend our up-to N^{3}LO HBChPT description of the $M1$ properties to $A = 3$ systems. By taking the magnetic moments of ^{3}H and ^{3}He as input to fix the coefficients of the contact-term operators, a completely parameter-free theory predictions will be made for the total cross section and the photon polarization of the thermal neutron capture process ($nd \to {}^3\mathrm{H}\gamma$). We will also revisit the theory predictions for the two-body observables: deuteron magnetic moment μ_d and σ_{np}.

The purpose of this article is to demonstrate the general tenet of EFTs by studying the $M1$ properties of a few-body systems: once the long-range contributions are taken into account correctly, EFTs enables accurate and model-independent results, regardless of the details of the short-range physics.

We begin with a few comments that are generic to all EFTs. At a certain order in EFTs, there appear contact terms (CTs), which parametrize the high-energy (or short-range) physics above the cutoff scale of the theory. The coefficients of CTs, which we refer to as low-energy constants (LECs), are thus sensitive to the short-range physics and depend on the adopted cutoff value and the regularization/renormalization scheme. The values of LECs are not fixed by the symmetry alone and should be determined by either solving the underlying theory or by fitting them so as to reproduce selected set of known experimental data. Because the former is currently not feasible, the latter remains the only practical option. At N^{3}LO, HBChPT $M1$ currents contain two nonderivative two-nucleon CTs, one in isovector and the other in isoscalar channel. These LECs, g_{4v} and g_{4s}, will be determined in this work by requiring to reproduce the experimental values of the magnetic moments of ^{3}H and ^{3}He. Once these LECs fixed, we are left with no free parameters and can make totally parameter-free theory predictions for the other $M1$ observables.[1] In EFTs, one should include all the terms up to the considered order. Omitting part of them can cause a cutoff dependence that is comparable to the contribution of the omitted operators [1–5,7–17].[2] In Ref. [1], the CT contributions have been ignored, causing small but noticeable cutoff dependence in σ_{np}. By taking into account of the LECs, we will show that σ_{np} becomes virtually completely cutoff independent. Second comment is about the accuracy of the adopted wave functions at short range. The authors of Ref. [16] have developed an approach called EFT* or MEEFT (*more effective* effective field theory) that enables a consistent and systematic EFT calculations on top of accurate

[*]yhsong@phy.duke.edu
[†]rimantas.lazauskas@ires.in2p3.fr
[‡]tspark@kias.re.kr

[1]There are many other alternatives. For example, one can fix g_{4v} and g_{4s} from the experimental values of σ_{np} and the deuteron magnetic moment μ_d and then make theory predictions on $\mu(^3\mathrm{H})$ and $\mu(^3\mathrm{He})$ [7].

[2]We remark that a similar observation has also been made for the nonperturbative renormalization of three-body states, showing that three-body contact interaction is needed to absorb the cutoff dependence [18].

but phenomenological wave functions. The key observations are following. The model dependence resides mainly in the short-range region of the wave functions. Because short-range contributions can be well embodied by local operators at low energy and because EFT has the machinery to contain all the relevant local operators (i.e., CTs) in a consistent and systematic manner, the model dependence due to short-range physics is to be absorbed into the renormalization procedure of the LECs. To be more specific, if we adopt other wave functions that have different short-range behavior, the values of LECs should also be changed so as to reproduce the selected experimental data *with* the adopted wave functions. By performing this procedure, while the values of LECs—which are not physical observables—are model dependent, the resulting net contributions become model independent. An easy and effective way of proving the model-independence in a quantitative fashion might be to look at the cutoff dependence of the results, because the cutoff value is the key parameter that characterizes the short-range contributions. Such a numerical proof will be taken in this work. The third comment is about the long-range contributions. Note that mismatches in the long-range contributions cannot be cured by finite set of local operators. The long-range part of the transition operator is usually governed by the chiral symmetry, leaving little uncertainty there. However, the long-range part of the wave functions is controlled by the effective range parameters (ERPs) such as the nuclear binding energies and the scattering lengths. For two-nucleon systems, most of the modern realistic NN potentials reproduce the ERPs with a great accuracy. However, for nucleon systems with $A \geqslant 3$, situation becomes highly nontrivial as many of the available potentials fail to reproduce the relevant ERPs to the desired accuracy.

As we will demonstrate, our results have little cutoff dependence for all the cases considered, which might be interpreted that the short-range physics is well under control. However, the model dependence due to the difference in long-range part of the wave functions will cause correlations of the matrix elements with the ERPs. In our work, we observe rather a strong model dependence and demonstrate how it is correlated to the model prediction of the triton binding energy B_3. It indicates that the model dependence is due to the mismatches in the long-range contributions.

To bypass the difficulty and to get model-independent accurate theory predictions, we have explored two different approaches. One is to bring prediction of B_3 to its experimental value $B_3^{\rm exp} = 8.482$ MeV, using the observed correlation curves. The resulting $M1$ matrix elements are found to be model independent to a good accuracy and consistent with the experimental data. Another way is to adjust the trinucleon interactions (TNIs) to meet the experimental values of the ERPs.

II. FORMALISM

A. Faddeev equations

During the past few decades several different methods to solve the three-body bound and scattering problem has been developed. In this study we solve Faddeev [19] equations (also often called Kowalski-Noyes equations) in configuration space to obtain three-body bound and scattering wave functions. We employ the isospin formalism, i.e., consider proton and neutron as two degenerate states of the same particle (nucleon), having the mass fixed to $\hbar^2/m = 41.471$ MeV fm. Then three Faddeev equations become formally identical, having the form

$$(E - H_0 - V_{ij})\Phi_{ij,k} = V_{ij}(\Phi_{jk,i} + \Phi_{ki,j}), \tag{1}$$

where (ijk) are particle indices, H_0 is kinetic energy operator, V_{ij} is two body force between particles i and j, $\Phi_{ij,k}$ is Faddeev component. It is useful to define cyclic (P^+) and anticyclic (P^-) particle permutation operators, which permits transformation of the Faddeev component between two particle bases: $P^+ = (P^-)^{-1} = P_{23}P_{12}$ and $P^+\Phi_{ij,k} = \Phi_{jk,i}$, while $P^-\Phi_{ij,k} = \Phi_{ki,j}$. The wave function in Faddeev formalism is the sum of three Faddeev components, which employing permutation operators can be written as:

$$\Psi = (1 + P^+ + P^-)\Phi_{ij,k}. \tag{2}$$

Faddeev components, if represented in its proper coordinate basis, have simple structure and analytical asymptotic behavior for the short-range potentials. We use relative Jacobi coordinates $\boldsymbol{x}_k = (\boldsymbol{r}_j - \boldsymbol{r}_i)$ and $\boldsymbol{y}_k = \frac{2}{\sqrt{3}}(\boldsymbol{r}_k - \frac{\boldsymbol{r}_i+\boldsymbol{r}_j}{2})$, whereas we expand Faddeev components on a bipolar harmonic basis:

$$\Phi_{ij,k} = \sum_\alpha \frac{F_\alpha(x_k, y_k)}{x_k y_k} |[l_x(s_i s_j)_{s_x}]_{j_x}(l_y s_k)_{j_y}\rangle_{\rm JM} \otimes |(t_i t_j)_{t_x} t_k\rangle_{TT_z}, \tag{3}$$

where index α represents all the symmetry allowed combinations of the quantum numbers presented in the brackets, l_x and l_y are the partial angular momenta associated with respective Jacobi coordinates, and s_i and t_i are the spins and isospins of the individual particles. Functionals $F_\alpha(x_k, y_k)$ are called partial Faddeev amplitudes. Three-nucleon system conserves its total angular momentum J as well as its projection M; however, due to the presence of charge-dependent terms in nuclear interaction, total isospin of the system T is not conserved.

Equation (1) is not complete, it should be complemented with the appropriate boundary conditions. Boundary conditions can be written in the Dirichlet form. First Faddeev amplitudes, for bound as well as for scattering states, satisfy the regularity conditions:

$$F_\alpha(0, y_k) = F_\alpha(x_k, 0) = 0. \tag{4}$$

For the bound-state problem wave function is compact, therefore the regularity conditions can be completed by forcing the amplitudes F_α to vanish at the borders of a hypercube $[0, X_{\rm max}] \times [0, Y_{\rm max}]$:

$$F_\alpha(X_{\rm max}, y_k) = F_\alpha(x_k, Y_{\rm max}) = 0. \tag{5}$$

Finally, we normalize three-nucleon wave function to unity $\langle\Psi \mid \Psi\rangle = 1$.

Faddeev components describing neutron-deuteron scattering, for the energies below the breakup threshold, vanish for $\mathbf{x}_k \to \infty$. As $\mathbf{y}_k \to \infty$ interaction between particle k and cluster ij is negligible and Faddeev components $\Phi_{jk,i}$ and $\Phi_{ki,j}$ vanish. Then the component $\Phi_{ij,k}$ describes the plane

wave of the particle k with respect to the bound particle pair ij:

$$\lim_{y_k\to\infty}\Phi_{ij,k}(\mathbf{x}_k,\mathbf{y}_k) = \frac{1}{\sqrt{3}}\sum_{j_n' l_n'}|\{\psi_d(\mathbf{x}_k)\}_{j_d}\otimes\{Y_{l_n}(\hat{\mathbf{y}}_k)\otimes s_k\}_{j_n}\rangle_{\rm JM} \otimes|(t_i t_j)_{t_d} t_k\rangle_{\frac{1}{2},-\frac{1}{2}}\frac{i}{2}\left[h_{l_n}^-(pr_{nd}) - S_{j_n l_n, j_n' l_n'}h_{l_n}^+(pr_{nd})\right], \quad (6)$$

where deuteron, being formed from nucleons i and j, has quantum numbers $s_d = 1$, $j_d = 1$, and $t_d = 0$ and its wave function $\psi_d(\mathbf{x}_k)$ is normalized to unity; p designates the relative momentum of incoming neutron, $r_{nd} = (\sqrt{3}/2)y_k$ is relative distance between neutron and deuteron target, whereas $h_{l_n}^{\pm}$ are the spherical Hankel functions. Expression (6) is normalized so that the nd scattering wave function has unity flux.

For zero or very low momentum neutrons, as is the case for the thermal neutron capture, only relative S-wave amplitudes survives in the asymptote, whereas expression (6) simplifies to:

$$\lim_{y_k\to\infty}\Phi_{ij,k}(\mathbf{x}_k,\mathbf{y}_k) = \frac{1}{\sqrt{3}}\sum_{j_n' l_n'}|\{\psi_d(\mathbf{x}_k)\}_{j_d}\otimes\{Y_{l_n}(\hat{\mathbf{y}}_k)\otimes s_k\}_{j_n}\rangle_{\rm JM} \otimes|(t_i t_j)_{t_d} t_k\rangle_{\frac{1}{2},-\frac{1}{2}}\left[1 - \frac{^{2J+1}a_{nd}}{r_{nd}}\right], \quad (7)$$

where $^{2J+1}a_{nd}$ is neutron-deuteron scattering length. For the cases where Urbana type three-nucleon interaction (TNI) are included, noting that the TNI among particles ijk can be written as sum of three terms $V_{ijk} = V_{ij}^k + V_{jk}^i + V_{ki}^j$, we modify the Faddeev equation (1) into:

$$(E - H_0 - V_{ij})\Phi_{ij,k} = V_{ij}(P^+ + P^-)\Phi_{ij,k} + \frac{1}{2}\left(V_{jk}^i + V_{ki}^j\right)\Psi. \quad (8)$$

B. Electromagnetic current

For a three-body system one has three one-body currents associated with each particle and three two-body currents associated with each pair of particles. Thus

$$J_{em} = \sum_{i=1, i\neq(j<k)}^{3}\left[J_{1B}^{(i)} + J_{2B}^{(jk)}\right]. \quad (9)$$

Because the wave functions $|\Psi\rangle$ in isospin formalism is fully antisymmetric, the matrix element of the current operators can be written as

$$\langle\Psi_f|J_{em}|\Psi_i\rangle = \sum_{i=1, i\neq(j<k)}^{3}\langle\Psi_f|J_{1B}^{(i)} + J_{2B}^{(jk)}|\Psi_i\rangle = 3\langle\Psi_f|J_{1B}^{(3)}|\Psi_i\rangle + 3\langle\Psi_f|J_{2B}^{(12)}|\Psi_i\rangle, \quad (10)$$

We use the electromagnetic current operators derived from HBchPT, which contain the nucleons and pions as pertinent degrees of freedom with all other massive fields integrated out. In HBchPT the electromagnetic currents and $M1$ operator are expanded systematically with increasing powers of Q/Λ_χ, where Q stands for the typical momentum scale of the process and/or the pion mass, $\Lambda_\chi \sim 4\pi f_\pi \sim m \sim 1$ GeV is the chiral scale, $f_\pi \sim 92.4$ MeV is the pion decay constant, and m is the nucleon mass. We remark that, while the nucleon momentum $\boldsymbol{p}$ is of order of Q, its energy ($\sim \frac{p^2}{m}$) is of order of Q^2/m, and consequently the four-momentum of the emitted photon $q^\mu = (\omega, \boldsymbol{q})$ with $|\boldsymbol{q}| = \omega$ also is counted as $O(Q^2/m)$. Current operators are obtained up to N^{3}LO. Note that three-body currents are N^{4}LO or higher order and do not enter in our work.[3]

Let us list the relevant current operators. The explicit form of magnetic moment operators can be found in Ref. [7]. The one-body current including the relativistic corrections reads

$$\begin{aligned} J_{1B}^{(i)}(\boldsymbol{q};\boldsymbol{r}_i) &= e^{-i\boldsymbol{q}\cdot\boldsymbol{r}_i}\left[\frac{Q_i}{m}\bar{\boldsymbol{p}}_i\left(1 - \frac{\bar{\boldsymbol{p}}_i^2}{2m}\right) + \frac{1}{2m}i\boldsymbol{q}\times\boldsymbol{\sigma}_i\left(\mu_i - \frac{Q_i}{2m^2}\bar{\boldsymbol{p}}_i^2\right)\right. \\ &\quad - \frac{\omega(2\mu_i - Q_i)}{8m^2}(2i\bar{\boldsymbol{p}}_i\times\boldsymbol{\sigma}_i) - \frac{\mu_i - Q_i}{16m^3}(4i\boldsymbol{q}\times\bar{\boldsymbol{p}}_i\boldsymbol{\sigma}_i\cdot\bar{\boldsymbol{p}}_i) \\ &\quad - \frac{w(2\mu_i - Q_i)}{8m^2}\boldsymbol{q} - \frac{\mu_i - Q_i}{16m^3}(-2\boldsymbol{q}\boldsymbol{q}\cdot\bar{\boldsymbol{p}}_i) \\ &\quad \left. + (\text{higher orders})\right], \end{aligned} \quad (11)$$

where Q_i and μ_i represent the charge and magnetic moment of i-th nucleon and $\bar{\boldsymbol{p}} \equiv \frac{1}{2}(i\overleftarrow{\nabla} - i\overrightarrow{\nabla})$ should be understood to act only on the nuclear wave functions.

Corrections to the 1B operator are due to the meson-exchange currents (MECs). Up to N^{3}LO, as mentioned, only two-body (2B) contributions enter (Figs. 1 and 2). It is to be emphasized that MECs derived in EFT are meaningful only up to a certain momentum scale characterized by the cutoff Λ. In our work, we adopt a Gaussian regulator in performing the Fourier transformation of the MECs from momentum space to coordinate space [16]. It is to be noted that the contributions due to high momentum exchanges (above the cutoff scale) are not simply ignored but, as we will discuss later, are accounted for by the renormalization of the contact-term coefficients.

We decompose the two-body current into the soft-one-pion-exchange (1π), vertex corrections to the one-pion exchange ($1\pi C$), the two-pion-exchanges (2π), and the contact-term (CT) contributions,

$$J_{2B}^{(jk)} = J_{1\pi}^{(jk)} + J_{1\pi C}^{(jk)} + J_{2\pi}^{(jk)} + J_{\rm CT}^{(jk)}. \quad (12)$$

It is noteworthy that there can be additional corrections to the two-body current coming from the so-called fixed term.

[3] It is worth mentioning that there is a different power counting scheme where the nucleon mass is regarded as heavier than the chiral scale, $m \sim \Lambda_\chi^2/Q$, see Ref. [20] for details. However, the use of this alternative counting scheme would not affect the results to be reported in this work because the difference between the two counting schemes would appear only at higher orders than explicitly considered here (N^{3}LO).

The fixed-term contributions represent vertex corrections to the soft-one-pion-exchange and fixed completely by Lorentz covariance. Because the fixed terms make the calculation highly involved, but give only very small contributions in $M1$ operator according to our previous study [7], we neglected the fixed term contributions in the present work.

The soft-one-pion exchange current $J_{1\pi}^{(jk)}$ is NLO and can be written in terms of $\boldsymbol{R}_{jk} = \frac{1}{2}(\boldsymbol{r}_j + \boldsymbol{r}_k)$, $\boldsymbol{r} = \boldsymbol{r}_j - \boldsymbol{r}_k$, $\hat{\boldsymbol{r}} = \boldsymbol{r}/|\boldsymbol{r}|$, $S_{jk} = 3\boldsymbol{\sigma}_j \cdot \hat{\boldsymbol{r}}\, \boldsymbol{\sigma}_k \cdot \hat{\boldsymbol{r}} - \boldsymbol{\sigma}_j \cdot \boldsymbol{\sigma}_k$,

$$
\begin{aligned}
&J_{1\pi}^{(jk)}(\boldsymbol{r}, \boldsymbol{R}) \\
&= e^{-i\boldsymbol{q}\cdot\boldsymbol{R}} \left\{ -\frac{g_A^2 m_\pi^2}{12 f_\pi^2} (\boldsymbol{\tau}_j \times \boldsymbol{\tau}_k)^z \boldsymbol{r} \left[\boldsymbol{\sigma}_j \cdot \boldsymbol{\sigma}_k \left(y_{0\Lambda}^{\pi}(r) - \frac{\delta_\Lambda(r)}{m_\pi^2} \right) \right.\right. \\
&\quad \left.\left. + S_{jk} y_{2\Lambda}^{\pi}(r) \right] + i \frac{g_A^2}{8 f_\pi^2} \boldsymbol{q} \times \left[\hat{T}_{S,jk}^{(\times)} \left(\frac{2}{3} y_{1\Lambda}^{\pi}(r) - y_{0\Lambda}^{\pi}(r) \right) \right. \right. \\
&\quad \left. \left. - \hat{T}_{T,jk}^{(\times)} y_{1\Lambda}^{\pi}(r) \right] \right\},
\end{aligned}
$$

where

$$
\begin{aligned}
\hat{T}_{S,jk}^{(\odot)} &= (\tau_j \odot \tau_k)^z (\boldsymbol{\sigma}_j \odot \boldsymbol{\sigma}_k), \\
\hat{T}_{T,jk}^{(\odot)} &= (\tau_j \odot \tau_k)^z \left[\hat{r}\, \hat{r} \cdot (\boldsymbol{\sigma}_j \odot \boldsymbol{\sigma}_k) - \tfrac{1}{3} (\boldsymbol{\sigma}_j \odot \boldsymbol{\sigma}_k) \right],
\end{aligned} \tag{13}
$$

$\odot = \pm, \times$, and the regulated delta and Yukawa functions are defined as

$$
\begin{aligned}
\delta_\Lambda(r) &\equiv \int \frac{d^3\boldsymbol{k}}{(2\pi)^3} e^{-k^2/\Lambda^2} e^{i\boldsymbol{k}\cdot\boldsymbol{r}} \\
y_{0\Lambda}^{\pi}(r) &\equiv \int \frac{d^3\boldsymbol{k}}{(2\pi)^3} e^{-k^2/\Lambda^2} e^{i\boldsymbol{k}\cdot\boldsymbol{r}} \frac{1}{\boldsymbol{k}^2 + m_\pi^2} \\
y_{1\Lambda}^{\pi}(r) &\equiv -r \frac{\partial}{\partial r} y_{0\Lambda}(r), \quad y_{2\Lambda}^{\pi}(r) \equiv \frac{r}{m_\pi^2} \frac{\partial}{\partial r} \frac{1}{r} \frac{\partial}{\partial r} y_{0\Lambda}(r).
\end{aligned} \tag{14}
$$

The one-loop vertex correction to the one-pion exchange has been investigated in detail in Refs. [1,2],

$$
\begin{aligned}
J_{1\pi\mathrm{C}}^{(12)} = e^{-i\boldsymbol{q}\cdot\boldsymbol{R}} i\boldsymbol{q} \times \Bigg\{ & -\frac{g_A^2}{8 f_\pi^2} (\bar{c}_\omega + \bar{c}_\Delta) \\
& \times \left[(\hat{T}_S^{(+)} + \hat{T}_S^{(-)}) \frac{\bar{y}_{0\Lambda}^{\pi}}{3} + (\hat{T}_T^{(+)} + \hat{T}_T^{(-)})\, y_{2\Lambda}^{\pi} \right] \\
& + \frac{g_A^2}{8 f_\pi^2} \bar{c}_\Delta \left[\frac{1}{3} \hat{T}_S^{(\times)} \bar{y}_{0\Lambda}^{\pi} - \frac{1}{2} \hat{T}_T^{(\times)} y_{2\Lambda}^{\pi} \right] \\
& - \frac{1}{16 f_\pi^2} \bar{N}_{WZ} \boldsymbol{\tau}_1 \cdot \boldsymbol{\tau}_2 \left[(\boldsymbol{\sigma}_1 + \boldsymbol{\sigma}_2) \bar{y}_{0\Lambda}^{\pi} \right. \\
& \left. + (3\hat{r}\hat{r} \cdot (\boldsymbol{\sigma}_1 + \boldsymbol{\sigma}_2) - (\boldsymbol{\sigma}_1 + \boldsymbol{\sigma}_2)) y_{2\Lambda}^{\pi} \right] \Bigg\},
\end{aligned} \tag{15}
$$

The values of the LECs $(\bar{c}_\omega, \bar{c}_\Delta, \bar{N}_{WZ})$ should in principle be fixed either by solving the underlying theory, QCD, or by fitting to suitable experimental observables. Because this has not yet been done, we adopt here the estimates given in Refs. [1, 2] based on the resonance saturation assumption and the Wess-Zumino action, $(\bar{c}_\omega, \bar{c}_\Delta, \bar{N}_{WZ}) \simeq (0.1021, 0.1667, 0.02395)$.

The two-pion exchange diagrams give rise to

$$
\begin{aligned}
J_{2\pi}^{jk} = \frac{e^{-i\boldsymbol{q}\cdot\boldsymbol{R}}}{128\pi^2 f_\pi^4} \Big\{ & i\boldsymbol{q} \times [(\hat{T}_S^{(+)} - \hat{T}_S^{(-)}) L_S(r) \\
& + (\hat{T}_T^{(+)} - \hat{T}_T^{(-)}) L_T(r)] - (\tau_j \times \tau_k)^z \hat{r} \frac{d}{dr} L_0(r) \Big\},
\end{aligned} \tag{16}
$$

where

$$
\begin{aligned}
L_S(r) &= -\frac{g_A^2}{3} r \frac{d}{dr} K_0 + \frac{g_A^4}{3} \\
&\quad \times \left(-2K_0 + 4K_1 + r \frac{d}{dr} K_0 + 2r \frac{d}{dr} K_1 \right) \\
L_T(r) &= \frac{g_A^2}{2} r \frac{d}{dr} K_0 + \frac{g_A^4}{2} \left(4K_{\mathrm{T}} - r \frac{d}{dr} K_0 - 2r \frac{d}{dr} K_1 \right) \\
L_0(r) &= 2K_2 + g_A^2 (8K_2 + 2K_1 + 2K_0) \\
&\quad - g_A^4 (16K_2 + 5K_1 + 5K_0) + g_A^4 \frac{d}{dr} (r K_1),
\end{aligned} \tag{17}
$$

and the loop functions K's are defined in Refs. [1,16].

Finally, contact-term contributions have the form

$$
J_{\mathrm{CT}}^{(jk)} = e^{-i\boldsymbol{q}\cdot\boldsymbol{R}} \frac{i}{2m_p} \boldsymbol{q} \times [g_{4S}(\boldsymbol{\sigma}_j + \boldsymbol{\sigma}_k) + g_{4V} T_S^{(\times)}] \delta_\Lambda(r) \tag{18}
$$

where $g_{4S} = m_p g_4$ and $g_{4V} = -m_p (G_A^R + \frac{1}{4} E_T^{V,R})$. We remark that three contact terms were introduced in Refs. [1,2], whose coefficients are denoted as g_4, G_A^R, and $E_T^{V,R}$. However, due to Fermi-Dirac statistics, only two of them are independent and consistent with Eq. (18). A similar reduction has been noticed for the Gamow-Teller operator, where only one linear combination of two CTs is required [16].

C. *n-d* radiative capture

In center-of-mass frame, each currents can be written in the form of

$$
J_{em} = e^{-i\boldsymbol{q}\cdot\boldsymbol{x}} (i\boldsymbol{q} \times \boldsymbol{j}_\mu + \boldsymbol{j}_c), \tag{19}
$$

where $\boldsymbol{x}$ is $\boldsymbol{r}_i$ for $J_{1B}^{(i)}$ and $\boldsymbol{R}_{jk}$ for $J_{2B}^{(jk)}$.

To calculate neutron radiative capture observables we will use multipole expansion. First we introduce a shorthand notations for the multipoles:

$$
\begin{aligned}
F_{\mathrm{JM}}(\hat{\boldsymbol{r}}) &= j_J(qr) Y_{\mathrm{JM}}(\hat{\boldsymbol{r}}), \\
F_{\mathrm{JL}}^M(\hat{\boldsymbol{r}}) &= j_L(qr) \mathcal{Y}_{JL1}^M(\hat{\boldsymbol{r}}),
\end{aligned} \tag{20}
$$

where $j_L(qr)$ is the spherical Bessel function; Y_{JM} and $\mathcal{Y}_{JL1}^M$ are spherical and vector-spherical harmonics, respectively; r is a vector describing the particle (nucleon or meson), which interacts with EM field. Then the electric and magnetic multipoles read

$$
\begin{aligned}
\mathcal{M}_{\mathrm{JM}} = F_{JJ}^M(\hat{\boldsymbol{r}}) \cdot \boldsymbol{j}_c + iq \Bigg[& \left(\frac{J+1}{2J+1} \right)^{1/2} F_{JJ-1}^M(\hat{\boldsymbol{r}}) \\
& - \left(\frac{J}{2J+1} \right)^{1/2} F_{JJ+1}^M(\hat{\boldsymbol{r}}) \Bigg] \cdot \boldsymbol{j}_\mu,
\end{aligned}
$$

$$\mathcal{E}_{\mathrm{JM}} = i\left[\left(\frac{J+1}{2J+1}\right)^{1/2} F^M_{JJ-1}(\hat{\boldsymbol{r}}) - \left(\frac{J}{2J+1}\right)^{1/2} F^M_{JJ+1}(\hat{\boldsymbol{r}})\right]\cdot \boldsymbol{j}_c + q\,F^M_{JJ}(\hat{\boldsymbol{r}})\cdot \boldsymbol{j}_\mu. \tag{21}$$

With the explicit expressions of the $F^M_{1L}(\hat{\boldsymbol{r}})$, $M1$ multipoles can also be written as

$$\mathcal{M}_{1M} = i\sqrt{\frac{3}{8\pi}}\, j_1(qr)(\hat{\boldsymbol{r}}\times \boldsymbol{j}_c) + \frac{iq}{\sqrt{6\pi}}\left\{ j_0(qr)\boldsymbol{j}_\mu - \frac{1}{2} j_2(qr)[\boldsymbol{j}_\mu - \hat{\boldsymbol{r}}(\hat{\boldsymbol{r}}\cdot \boldsymbol{j}_\mu)]\right\}. \tag{22}$$

In terms of the reduced matrix elements (RMEs) [21,22],

$$\widetilde{\mathcal{X}}^{J_i J_f}_J = \frac{\sqrt{6\pi}}{q\mu_N}\sqrt{4\pi}\left\langle \Psi^{J_f}_{\mathrm{b.s.}} \middle\| \mathcal{X}_{\mathrm{JM}} \middle\| \Psi^{J_i}_{\mathrm{scat}}\right\rangle, \tag{23}$$

where $\mathcal{X}_{\mathrm{JM}} = (\mathcal{M}_{\mathrm{JM}}, \mathcal{E}_{\mathrm{JM}})$, the total nd capture cross section is given by

$$\sigma_{nd} = \frac{2}{9}\frac{\alpha}{(v_{\mathrm{rel}}/c)}\left(\frac{\hbar c}{2mc^2}\right)^2\left(\frac{q}{\hbar c}\right)^3 \times \sum_{J_i}\sum_{J=1}^{J_i+\frac{1}{2}}\left(\left|\widetilde{\mathcal{E}}^{J_i,\frac{1}{2}}_J\right|^2 + \left|\widetilde{\mathcal{M}}^{J_i,\frac{1}{2}}_J\right|^2\right). \tag{24}$$

Thermal neutron capture proceeds only from doublet $J^\Pi_i = \frac{1}{2}^+$ and quartet $J^\Pi_i = \frac{3}{2}^+ nd$ scattering states, because only these two states comprise nd S-wave asymptote and thus dominate low-energy scattering. Because final state (the triton) is $J^\Pi_f = \frac{1}{2}^+$, therefore only magnetic dipole transition elements $m_2 \equiv \widetilde{\mathcal{M}}^{\frac{1}{2},\frac{1}{2}}_1$, $m_4 \equiv \widetilde{\mathcal{M}}^{\frac{3}{2},\frac{1}{2}}_1$ and electric quadrupole transition element $e_4 \equiv \widetilde{\mathcal{E}}^{\frac{3}{2},\frac{1}{2}}_2$ do not vanish. Notice that magnetic dipole moments are purely imaginary, while the electric quadrupole moment is real.

Experimentally, in addition to capture cross section, photon polarization parameter R_c can also be measured. This parameter is given by Ref. [22]

$$R_c = \frac{1}{3}\left[\frac{\frac{7}{2}|m_4|^2 + \sqrt{8}\mathrm{Re}(m_2 m_4^*) + \frac{5}{2}|e_4|^2 + \sqrt{24}\mathrm{Im}(m_2 e_4^*) - \sqrt{3}\mathrm{Im}(m_4 e_4^*)}{|m_2|^2 + |m_4|^2 + |e_4|^2} - 1\right]. \tag{25}$$

Calculations using expression (10) are numerically stable for all the two- and one-body current terms except the ones entering into impulse approximation of the $M1$ operator. This issue has been observed and the special numerical procedure developed in Ref. [23]; we have successfully followed it.

III. RESULTS

A. Binding energies and scattering lengths

In this work we have performed rigorous calculations for several qualitatively different realistic nuclear Hamiltonians, which are based on NN potentials defined both in configuration and momentum spaces. Argonne Av18 [24] is an accurate local NN potential in configuration space. Semirealistic configuration space potential INOY has been recently derived by Doleschall [25], which can describe binding energies of three-nucleon systems with only two-nucleon forces. ISUJ [26]—a recent revision of INOY—further improves description of np and pp data and at low energies provides solution for the long-standing "Ay puzzle" of N-d scattering. We have also tested some chiral N^{3}LO potentials defined in momentum space: Idaho group potential [27] (referred to as I-N^{3}LO), and three different parametrizations of chiral N^{3}LO potential of Bonn-Bochum group [20]. In particular Bonn-Bochum group potentials parameterized with set of cutoff values $\{\Lambda, \widetilde{\Lambda}\} = \{450, 500\}$, $\{450, 700\}$, and $\{600, 700\}$ MeV have been used and are referred to as B1-N^{3}LO, B2-N^{3}LO, and B3-N^{3}LO, respectively.

All the NN potentials mentioned above describe the NN data quite accurately. And all but Bonn-Bochum group potentials reproduce experimental deuteron binding energy B_d and the singlet np scattering length $^1a_{np}$ with at least four significative digit accuracy. Values of these observables obtained using Bonn-Bochum group potentials are summarized in Table I.

Our three-body calculations have been carried out considering isospin breaking effects, which allow admixture of total isospin $T = 3/2$ in the wave functions. The Argonne UIX three-nucleon interaction [28] also has been taken into account in the combination with Av18 NN potential.

The relevant properties of three-body systems obtained with the adopted models are summarized in Table II. These values are in perfect agreement with ones obtained by the other

TABLE I. Values for np singlet scattering length and deuteron binding energy obtained using Bonn-Bochum group potentials.

Model	$^1a_{np}$ (fm)	B_{H_2} (MeV)
B1-N^{3}LO	−23.60	2.215
B2-N^{3}LO	−23.72	2.218
B3-N^{3}LO	−23.64	2.220
Exp.	−23.74	2.225

TABLE II. Three-nucleon properties as calculated with different realistic Hamiltonians. They contain: nd doublet ($^2a_{nd}$) and quartet ($^4a_{nd}$) scattering lengths in fm; bound-state properties comprising binding energy (BE), average kinetic energy ($\langle T\rangle$) in MeVs, and rms radius $r_{\rm rms} = \sqrt{\langle r^2\rangle}$ in fm. These values are compared to other theoretical calculations and experimental results.

Hamiltonian	Ref.	nd		^{3}H			^{3}He		
		$^2a_{nd}$	$^4a_{nd}$	BE	$\langle T\rangle$	$r_{\rm rms}$	BE	$\langle T\rangle$	$r_{\rm rms}$
Av18	This work	1.266	6.331	7.623	46.71	1.769	6.925	45.67	1.810
	[29,31]	1.248	6.346	7.623(2)			6.924(1)		
Av18+UIX	This work	0.598	6.331	8.483	51.29	1.683	7.753	50.23	1.716
	[29,31]	0.578	6.347	8.478(2)			7.748(2)		
INOY	This work	0.551	6.331	8.483	33.00	1.666	7.720	32.22	1.704
	[25]			8.482			7.718		
ISUJ	This work	0.523	6.330	8.484	32.95	1.667			
	[26]			8.482			7.718		
I-N^{3}LO	This work	1.101	6.337	7.852	34.54	1.760	7.159	33.83	1.797
	[32]			7.854					
B1-N^{3}LO	This work	1.263	6.334	7.636	33.60	1.816	6.904	32.79	1.860
	[33]			7.64					
B2-N^{3}LO	This work	1.024	6.339	7.930	31.70	1.777	7.210	31.01	1.815
	[33]			7.97					
B3-N^{3}LO	This work	1.781	6.329	7.079	47.25	1.863	6.403	46.17	1.909
	[33]			7.09					
Exp.		0.65 ± 0.04 [30]	6.35 ± 0.02 [30]	8.482	–		7.718	–	

groups [25,29,31–33]. In Ref. [34] we have already published three-nucleon properties for INOY and Av18 models, the small difference in fourth digit of those results compared with current ones is due to the small admixture of isospin $T = 3/2$ states. One should note that only INOY, ISUJ, and Av18+UIX models reproduce experimental three-nucleon binding energies as well as neutron-deuteron doublet ($J = \frac{1}{2}$) scattering length accurately. Chiral potentials at N^{3}LO comprise already two irreducible three-nucleon interaction diagrams with contact terms. The strength of these contact terms may be *a priori* adjusted so as to reproduce three-nucleon binding energy and scattering length [35]. In this work, however, only two-nucleon interaction part of N^{3}LO models was considered.

B. Magnetic moments and thermal neutron capture

In Table III, we present $M1$ RMEs obtained for INOY Hamiltonians with $\Lambda = 700$ MeV, listing the contributions from each chiral order. Note that the one-body contribution of the isoscalar $M1$ RME, m_2, is strongly suppressed due to the pseudo-orthogonality between initial- and final-wave functions. The chiral convergence is, however, not much illuminating, i.e., N^{3}LO contributions appear about the same size of NLO. This behavior is mainly due to the accidental cancellation between two NLO contributions, the seagull and pion-pole diagrams [36].

As explained, $M1$ currents contain two nonderivative contact terms at N^{3}LO. Because the coefficients of them, g_{4S} and g_{4V}, cannot be determined from the underlaying theory yet, we fit these constants by requiring that magnetic moments of ^{3}H and ^{3}He are correctly reproduced. The resulting values obtained with INOY potential are given in Table IV. We remark that g_{4S} and g_{4V} depend on cutoff Λ as well as on particular choice of nuclear Hamiltonian.

Table V shows the cutoff dependence of our results. One-body contributions are cutoff independent by their construction. NLO results bring sizable cutoff dependence, indicating that some important pieces are omitted at this level. As is

TABLE III. Matrix elements calculated for magnetic moments and thermal neutron capture. These results are obtained using INOY Hamiltonians with $\Lambda = 700$ MeV.

	$\mu(^2\mathrm{H})$	$\mu(^3\mathrm{H})$	$\mu(^3\mathrm{He})$	$\frac{1}{i}\widetilde{\mathcal{M}}_1^{0,1}$	$\frac{1}{i}\widetilde{\mathcal{M}}_1^{\frac{1}{2},\frac{1}{2}}$	$\frac{1}{i}\widetilde{\mathcal{M}}_1^{\frac{3}{2},\frac{1}{2}}$	$\widetilde{\mathcal{E}}_2^{\frac{3}{2},\frac{1}{2}}$
LO: 1B	0.8593	2.6567	−1.8100	395.5000	−13.6196	13.1149	−0.0741
N^{3}LO: 1B	−0.0057	−0.0199	0.0080	−0.1653	0.4106	0.1048	0.0032
NLO: 1π	0.0000	0.1515	−0.1501	7.0970	−2.5712	−0.4289	0.1562
N^{3}LO: $1\pi C$	−0.0029	0.0839	−0.0926	3.1860	−2.7674	−0.3465	0.0000
N^{3}LO: 2π	0.0000	0.0374	−0.0362	1.1290	−1.2504	−0.1223	−0.0019
g_{4S}	0.0338	0.0457	0.0449	0.0000	−0.9855	0.2647	0.0000
g_{4V}	0.0000	0.0733	−0.0712	2.3130	−2.5179	−0.2267	0.0000

TABLE IV. Values of contact term coefficients g_{4s} and g_{4V} , which are obtained by fitting magnetic moments of triton and ^{3}He, for INOY Hamiltonians.

Λ (MeV)	g_{4s}	g_{4V}
500	0.2747	1.8746
700	0.2313	0.8021
900	0.1997	0.4613

indicated in the table, going N^{3}LO but without taking the CTs does not help in resolving the situation. It is only after the CTs taken into account that the results become almost independent of the cutoff, which implies that the CTs are quite effective in renormalizing away the details residing in the short-range region.

Results with varying model Hamiltonians are given in Table VI, with some relevant low-energy properties of the potentials. From the table, one observes that $\mu(^2\mathrm{H})$ and σ_{np} are rather insensitive, R_c is moderately sensitive and the nd capture cross section, σ_{nd}, is highly sensitive on the model Hamiltonian. To understand the sensitivity, let us consider the model dependence of the effective-range parameters (ERPs), which govern the long-range part of the RMEs. The most important ERPs are the binding energies and the scattering lengths, which should strongly influence $M1$ RMEs through the coupling of the long-range parts of the three-nucleon wave functions. And indeed, as shown in Fig. 3, the $M1$ RMEs are strongly correlated with the triton binding energy B_3. The correlation is found to be almost perfect for m_4, while with some fluctuation for m_2. These behavior can be explained with simple arguments: let us first concentrate on the quartet RME, m_4. In spin-quartet states, Pauli principle inhibits three nucleons from gathering altogether, and thus observables are insensitive to short-range part of three-nucleon interaction. As a result, the nd quartet scattering length $^4a_{nd}$ has little model dependence; all the models considered here reproduce $^4a_{nd}$ in excellent agreement with the experimental data. This explains the perfect correlation of m_4 with B_3. On the contrary, spin-doublet states are free from the exclusion principle and sensitive to the short-range three-nucleon interaction. This makes the scattering length $^2a_{nd}$ largely model dependent (see Table VI), and we might expect that m_2 depends not only on B_3 but also on $^2a_{nd}$. However, $^2a_{nd}$ and B_3 are correlated, which is known in terms of the Phillips line [37].[4] The correlation of $^2a_{nd}$ with B_3 is not perfect, showing small deviations from the Phillips line. These arguments are in good accordance with what we observe in Fig. 3, which shows the correlation of m_2 with respect to B_3 with some scatters.

For noble two-body processes, the effective range expansion technique often allows an even algebraic relation of the RMEs in terms of ERPs; see, for example, Ref. [17] for the Gamow-Teller matrix element of the $p + p \to d + e^+ + \nu$ process. The problem at hand is, however, too complicated to allow such mathematical rigor, and we will limit ourselves to an empirical curve fitting. We take the trial function as

$$m_n^{(i)} \simeq \phi_n\big[B_3^{(i)}\big] \tag{26}$$

with

$$\phi_n(B_3) = m_n^0 + t_n\big[\big(B_3/B_3^{\mathrm{exp}}\big)^{\nu} - 1\big], \tag{27}$$

where the superscript i is the model index; that is, $m_n^{(i)}(n = 2, 4)$ and $B_3^{(i)}$ stands for the RMEs and ^{3}H BE obtained with the i-th model potential, respectively. Varying the value of ν, values of m_n^0 and t_n are searched by a χ^2 fit. The resulting χ^2 is found to be parabola shape with minimum at around $\nu = -2.5$. The solution with $\nu = -2.5$ is

$$\begin{aligned}\phi_2(B_3) &= (-21.87 \pm 0.24) - 10.76\big[\big(B_3/B_3^{\mathrm{exp}}\big)^{-2.5} - 1\big],\\ \phi_4(B_3) &= (12.24 \pm 0.05) + 11.35\big[\big(B_3/B_3^{\mathrm{exp}}\big)^{-2.5} - 1\big].\end{aligned} \tag{28}$$

[4] See, for example, Ref. [18] for the discussion of the Phillips line in the context of modern EFT.

TABLE V. Dependence of $M1$ observables for two- and three-nucleon systems on cutoff value Λ. These results are obtained using INOY Hamiltonians.

Λ (MeV)	$\mu(^2\mathrm{H})$	$\mu(^3\mathrm{H})$	$\mu(^3\mathrm{He})$	σ_{np} (mb)	σ_{nd} (mb)	R_c
			LO			
–	0.8593	2.657	−1.810	309.7	0.2785	−0.2369
			NLO			
500	0.8593	2.760	−1.913	318.7	0.2972	−0.3026
700	0.8593	2.808	−1.960	320.9	0.3296	−0.3538
900	0.8593	2.829	−1.980	321.9	0.3480	−0.3753
			N^{3}LO without contact term			
500	0.8499	2.836	−2.011	324.1	0.3612	−0.3896
700	0.8507	2.910	−2.081	327.5	0.4237	−0.4366
900	0.8515	2.937	−2.105	328.8	0.4526	−0.4504
			N^{3}LO			
500	0.8584	2.9790	−2.1276	330.9	0.5012	−0.4659
700	0.8585	2.9790	−2.1276	330.5	0.4946	−0.4649
900	0.8583	2.9790	−2.1276	330.4	0.4959	−0.4650
Exp.	0.8574	2.9790	−2.1276	332.6 ± 0.7	0.508 ± 0.015	−0.420 ± 0.030

TABLE VI. Predictions for the deuterons magnetic moment and the observables of the thermal neutron capture on protons and deuterons. These calculations have been realized by fixing contact terms of the meson exchange current to reproduce magnetic moments of the triton and ^{3}He. These values turns to be insensitive to the cutoff parameter in the interval $\Lambda = (500, 900)$ MeV; if, however, variation was larger than one affecting the fourth significant digit it is given in parentheses. The constructed Av18+UIX* model gives $^2a_{nd} = 0.623$ fm, $^4a_{nd} = 6.331$ fm and BE(^{3}He) = 7.718 MeV; the I-N^{3}LO+UIX** results are $^2a_{nd} = 0.634$ fm, $^4a_{nd} = 6.339$ fm and BE(^{3}He) = 7.737 MeV. Both these models are adjusted to reproduce experimental triton binding energy of BE(^{3}H) = 8.482 MeV.

Model	$\mu(^2\mathrm{H})$	σ_{np} (mb)	σ_{nd} (mb)	R_c
Av18	0.8575	331.9(1)	0.680(3)	−0.435
Av18+UIX	0.8604	330.6(2)	0.478(3)	−0.458
INOY	0.8585	330.6(2)	0.498(3)	−0.465
ISUJ	0.8585	331.1(2)	0.501(2)	−0.466
I-N^{3}LO	0.8574	330.4(3)	0.626(2)	−0.441
B1-N^{3}LO	0.8577	328.7(6)	0.688(4)	−0.438(1)
B2-N^{3}LO	0.8588	331.0(4)	0.609(4)	−0.448(1)
B3-N^{3}LO	0.8549	330.9(7)	0.879(8)	−0.411(2)
Av18+UIX*	0.8614(1)	330.9(3)	0.476(2)	−0.457(1)
I-N^{3}LO+UIX**	0.8590(1)	329.7(3)	0.477(3)	−0.468(1)
Exp.	0.8574	332.6 ± 0.7 [38]	0.508 ± 0.015 [39]	−0.420 ± 0.030 [40]

The solution is drawn in solid line in the figure. The above curve fitting procedure turns out to be quite robust. For example, the curves and the values of m_n^0 with $\nu = -1.5$ are almost the same as those with $\nu = -2.5$. Even if we try a simple-minded linear fit, $\nu = 1$, we have $\phi_2(B_3) = -21.73 + 33.65(x_3 - 1)$ and $\phi_4(B_3) = 12.14 - 35.69(x_3 - 1)$, $x_3 \equiv E_{\mathrm{H3}}/E_{\mathrm{H3}}^{\mathrm{exp}}$. Thus the values of $\phi_n(B_3^{\mathrm{exp}}) = m_n^0$ are quite insensitive to the fitting parameter ν. Furthermore, with the resulting values of $\phi_n(B_3^{\mathrm{exp}}) = m_n^0$, we have $R_c = -0.462 \pm 0.03$ and $\sigma_{nd} = 0.490 \pm 0.008$ mb, which are close to the experimental data. Therefore one can conclude that the observed strong model dependence in $M1$ properties of three-body systems can be traced to the different model predictions of B_3 and that, once we have correct B_3, the theory predictions should be very close to the experimental data with little model dependence.

We have also tried to adjust the nuclear potentials to have correct ERPs. As mentioned, B_3 and $^2a_{nd}$ are the relevant ERPs. But because the two ERPs are strongly correlated to each other, simultaneous reproduction of both is rather tricky. This correlation in particular strong due to on-shell NN interaction part, nevertheless three-nucleon interaction can break it. Note that UIX TNI potential consists of two terms. In our calculation, we have readjusted the parameters of those terms to reproduce B_3 and $^2a_{nd}$ simultaneously with the Av18 and I-N^{3}LO NN potential. We refer, respectively, to the resulting Hamiltonians as Av18+UIX* and I-N^{3}LO+UIX**. In addition some charge dependence has been added to UIX*, permitting Av18+UIX* to reproduce also ^{3}He binding energy. The corresponding results are given in the bottom lines of the Table VI. The most important observation to be made is that, while the results of Av18, Av18+UIX, and I-N^{3}LO differ dramatically, the modified Hamiltonians Av18+UIX* and I-N^{3}LO+UIX** give us almost identical results, which confirms the argument that our theory predictions are model independent once the ERPs are correctly encoded. The resulting σ_{nd} and R_c are close to the experimental data, but with discrepancy of about two σs of the data.

Before closing this section, we compare with other calculations for the processes considered in this article. Viviani *et al.* [41,42] has calculated the $M1$ properties of $A = 2$, 3 systems with the currents deduced from the adopted nuclear potentials using gauge invariance, adding model-dependent pieces for those part that are not fixed by the gauge symmetry alone. Their results have some variations depending on the adopted potentials [41] and the details of the treatment of the currents. Without model-dependent current part capture cross section is underestimated $\sigma_{nd} = (0.418 \sim 0.462)$ mb, nevertheless one gets $R_c = -(0.429 \sim 0.446)$ quite close to experimental value [42]. Model-dependent currents enable reproduction of the experimental cross section; however, the photon polarization parameter $R_c = -(0.469)$ becomes larger

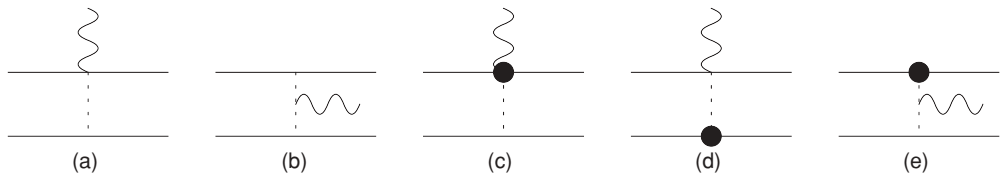

FIG. 1. Tree diagrams for the electromagnetic current operators. Soft one-pion-exchange, the sum of the "seagull" (a) and the "pion-pole" (b) diagrams contribute to the $J_{1\pi}$. Diagrams (c)–(e) contribute to the $J_{1\pi C}$ at N^{3}LO. The dot represents the vertex corrections coming from NLO or N^{2}LO Lagrangian.

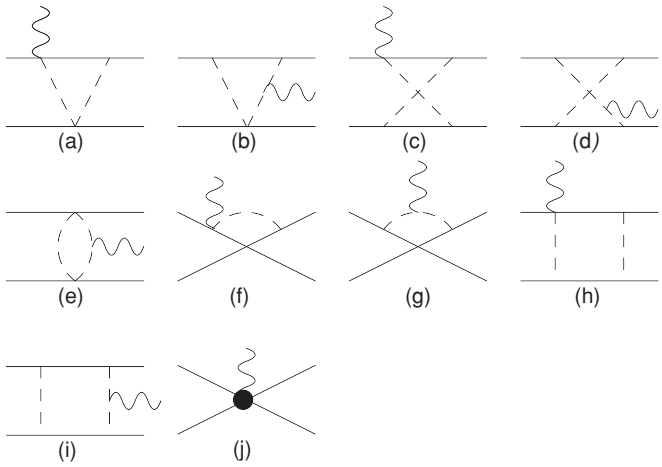

FIG. 2. Diagrams that contribute to $J_{2\pi}$(a)–(i) and $J_{\rm CT}$(j) at N^{3}LO.

than that of the experimental data. Currents related with three-nucleon force further increase capture cross section and photon polarization parameters. A result very similar to our calculation has been recently achieved by Pastore *et al.* [43], in which electromagnetic current operators have been obtained up to N^{3}LO within the EFT framework. Δ-isobar as well as pions and nucleons are treated as pertinent degrees of freedom. And they have applied the currents up to N^{2}LO to $A = 2$ and $A = 3$ systems. To this order, the CT terms—that play a crucial role in removing the model dependence at short-range physics—do not appear, and they have observed a large cutoff dependence with substantial underpredictions for σ_{nd} and

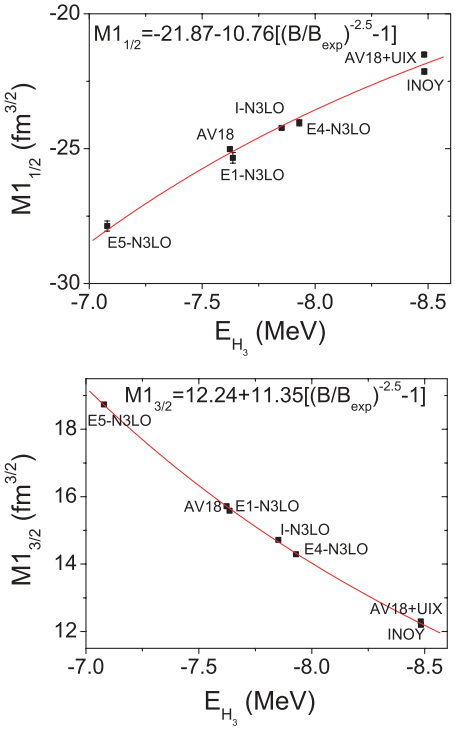

FIG. 3. (Color online) Radiative capture of thermal neutron by deuteron: correlation of $M1$ doublet and quartet RME's with triton binding energy.

R_c, $\sigma_{nd} = (0.450 \sim 0.315)$ mb and $R_c = -(0.437 \sim 0.331)$ for the momentum cutoff $\Lambda = (500 \sim 800)$ MeV. We also acknowledge that, using the so-called pionless EFT approach, Sadeghi *et al.* [5] have performed up to N^{2}LO (in their counting scheme) calculation for the σ_{nd} and R_c, achieving a perfect agreement with the data. In their calculations, the np cross section as well as the nd scattering lengths and the binding energies (of $A = 2$ and $A = 3$ systems) are taken as inputs needed to fix their parameters, the magnetic moments have not been considered. Because magnetic moments are sensitive to the D-wave components of the wave functions, it may not be trivial to have accurate theory predictions for the magnetic moments using the pionless EFT. A further study in this issue will be extremely interesting.

IV. DISCUSSIONS

The most natural candidate for the remaining small discrepancy might be the three-body current contributions, which are N^{4}LO. It is not difficult to notice that the leading three-body contributions are suppressed for both $M1$ currents and the nuclear potentials [18,44,45], for exactly the same reason. Furthermore, the soft one-pion-exchange appears as the leading two-body contributions for both of them. Thus we expect that the ratio of the three-body contribution to the two-body contribution is the same order for the $M1$ RMEs and the nuclear potentials,

$$\frac{\mathcal{M}_{\rm 3B}}{\mathcal{M}_{\rm 2B}} \sim \frac{\langle V\rangle_{\rm 3B}}{\langle V\rangle_{\rm 2B}} \sim (0.05 \sim 0.1). \tag{29}$$

Because the TNIs play a crucial role in reproducing the ERPs of three-body systems accurately, we may naively guess that the same will also be true for the relation between three-body currents and the $M1$ properties. More quantitatively, Eq. (29) with Table III tells us that the three-body current contribution will be about $(2 \sim 4)\%$ for m_2 and m_4, which is just the needed size to remove the discrepancy of σ_{nd} and R_c. The same has been demonstrated by Viviani *et al.* [42], where three-nucleon currents have let to increase neutron thermal capture cross section by 0.033 mb. In this regard, taking into account the three-body current contribution—while ignoring other pieces of N^{4}LO for simplicity—might be extremely interesting.

V. CONCLUSION

In this article $M1$ properties, comprising magnetic moments and radiative capture of thermal neutron observables are studied in two- and three-nucleon systems. We utilize meson exchange current derived up to N^{3}LO using heavy baryon chiral perturbation theory à la Weinberg. At N^{3}LO, two unknown parameters, g_{4s} and g_{4v}, enter as the coefficients of contact terms. Following the MEEFT strategy, we have fixed them by imposing the renormalization condition that the magnetic moments of tritium and ^{3}He are reproduced. Then we analyze the predictions for other $M1$ properties: magnetic moment of deuteron, as well as observables of the thermal neutron capture on proton and deuteron. Analysis comprises several qualitatively different realistic nuclear Hamiltonians,

which allows us to judge the model dependence of our results. We obtain stable, cutoff independent results, which reconfirms efficiency of MEEFT procedure. Model predictions for two-body observables (deuteron magnetic moment and thermal np capture cross section) scatter closely around the experimentally measured values.

Radiative capture cross section of thermal neutron on deuterons varies quite a bit from one Hamiltonian to the other. We have demonstrated that this variation is mostly due to the correlation of the capture cross section with a model-predicted three-nucleon binding energy. By fixing three-nucleon binding energy to the experimental value one can reduce model dependence below a 2% level and obtain model-independent predictions for thermal capture cross section $\sigma_{nd} = 0.490 \pm 0.008$ mb and photon polarization parameter $R_c = -0.462 \pm 0.03$. Within these model-dependent error bars capture cross section agrees with experimentally measured value 0.508 ± 0.015 mb [39]. However, the photon polarization parameter R_c is obtained slightly too large, like in other studies based on realistic nuclear Hamiltonians and currents [42]. The remaining discrepancy is comparable in size with higher-order terms of the EFT, which have been neglected here. We believe that in particular three-nucleon currents, which first appear at N^4LO in our power counting scheme, should be important.

ACKNOWLEDGMENTS

The work of TSP was supported by the KOSEF Basic Research Program with the Grant No. R01-2006-10912-0 and by the KOSEF grant funded by the Korea Government (MEST) (No. M20608520001-08B0852-00110). The numerical calculations have been performed at IDRIS (CNRS, France). We thank the staff members of the IDRIS computer center for their constant help. TSP is grateful to Prof. Daniel Phillips and Prof. Seung-Woo Hong for valuable discussions. Last but not least we would like to thank Prof. Mannque Rho for his kindness accepting to read the manuscript prior to its publication and giving us important comments.

[1] T.-S. Park, D.-P. Min, and M. Rho, Phys. Rev. Lett. **74**, 4153 (1995); Nucl. Phys. **A596**, 515 (1996); T.-S. Park, K. Kubodera, D.-P. Min, and M. Rho, Phys. Rev. C **58**, R637 (1998).
[2] T.-S. Park, K. Kubodera, D.-P. Min, and M. Rho, Phys. Lett. **B472**, 232 (2000).
[3] C. H. Hyun,T.-S. Park, and D.-P. Min, Phys. Lett. **B516**, 321 (2001).
[4] J.-W. Chen and M. J. Savage, Phys. Rev. C **60**, 065205 (1999); J.-W. Chen, G. Rupak, and M. J. Savage, Phys. Lett. **B464**, 1 (1999).
[5] H. Sadeghi and S. Bayegan, Nucl. Phys. **A753**, 291 (2005); H. Sadeghi, S. Bayegan, and H. W. Griesshammer, Phys. Lett. **B643**, 263 (2006); H. Sadeghi, Phys. Rev. C **75**, 044002 (2007).
[6] R. Skibiński, J. Golak, H. Witala, W. Glöckle, A. Nogga, and E. Epelbaum, Acta Phys. Pol. B **37**, 2905 (2006).
[7] Y.-H. Song, R. Lazauskas, and T.-S. Park, Phys. Lett. **B656**, 174 (2007).
[8] T.-S. Park, D.-P. Min, and M. Rho, Phys. Rep. **233**, 341 (1993); T.-S. Park, I. S. Towner, and K. Kubodera, Nucl. Phys. **A579**, 381 (1994).
[9] T.-S. Park, H. Jung, and D.-P. Min, Phys. Lett. **B409**, 26 (1997); J. Korean Phys. Soc. **41**, 195 (2002).
[10] G. P. Lepage, nucl-th/9706029; T.-S. Park, D.-P. Min, and M. Rho, Nucl. Phys. **A646**, 83 (1999); C. H. Hyun, D.-P. Min, and T.-S. Park, Phys. Lett. **B473**, 6 (2000); T.-S. Park, K. Kubodera, D.-P. Min, and M. Rho, Nucl. Phys. **A684**, 101 (2001); T.-S. Park, Mod. Phys. Lett. A **22**, 2143 (2007).
[11] S. Ando, T.-S. Park, and D.-P. Min, Phys. Lett. **B509**, 253 (2001).
[12] T.-S. Park, K. Kubodera, and F. Myhrer, Phys. Lett. **B533**, 25 (2002).
[13] D. Gazit, Phys. Lett. **B666**, 472 (2008).
[14] S. Nakamura *et al.*, Nucl. Phys. **A707**, 561 (2002); **A721**, 549 (2003); S. Ando, Y. H. Song, T.-S. Park, H. W. Fearing, and K. Kubodera, Phys. Lett. **B555**, 49 (2003).
[15] J.-W. Chen, G. Rupak, and M. J. Savage, Nucl. Phys. **A653**, 386 (1999); M. Butler and J.-W. Chen, *ibid.* **A675**, 575 (2000); M. Butler, J.-W. Chen, and X. Kong, Phys. Rev. C **63**, 035501 (2001).
[16] T.-S. Park, L. E. Marcucci, R. Schiavilla, M. Viviani, A. Kievsky, S. Rosati, K. Kubodera, D. P. Min, and M. Rho, Phys. Rev. C **67**, 055206 (2003); K. Kubodera and T.-S. Park, Annu. Rev. Nucl. Part. Sci. **54**, 19 (2004).
[17] T.-S. Park, K. Kubodera, D.-P. Min, and M. Rho, Astrophys. J. **507**, 443 (1988).
[18] P. F. Bedaque, H. W. Hammer, and U. van Kolck, Phys. Rev. Lett. **82**, 463 (1999); Nucl. Phys. **A676**, 357 (2000).
[19] L. D. Faddeev, Zh. Eksp. Teor. Fiz. **39**, 1459 (1960) [Sov. Phys. JETP **12**, 1014 (1961)].
[20] E. Epelbaum, W. Glöckle, and U.-G. Meissner, Nucl. Phys. **A747**, 362 (2005); **A671**, 295 (2000).
[21] J. Carlson and R. Schiavilla, Rev. Mod. Phys. **70**, 743 (1998).
[22] M. Viviani, R. Schiavilla, and A. Kievsky, Phys. Rev. C **54**, 534 (1996).
[23] J. L. Friar, B. F. Gibson, and G. L. Payne, Phys. Lett. **B251**, 11 (1990).
[24] R. B. Wiringa, V. G. J. Stoks, and R. Schiavilla, Phys. Rev. C **51**, 38 (1995).
[25] P. Doleschall, I. Borbély, Z. Papp, and W. Plessas, Phys. Rev. C **67**, 064005 (2003).
[26] P. Doleschall, Phys. Rev. C **77**, 034002 (2008).
[27] D. R. Entem and R. Machleidt, Phys. Rev. C **68**, 041001(R) (2003).
[28] B. S. Pudliner, V. R. Pandharipande, J. Carlson, and R. B. Wiringa, Phys. Rev. Lett. **74**, 4396 (1995).
[29] H. Witala, A. Nogga, H. Kamada, W. Glöckle, J. Golak, and R. Skibinski, Phys. Rev. C **68**, 034002 (2003).
[30] W. Dilg, L. Koester, and W. Nistler, Phys. Lett. **B36**, 208 (1971).
[31] A. Nogga, A. Kievsky, H. Kamada, W. Glöckle, L. E. Marcucci, S. Rosati, and M. Viviani, Phys. Rev. C **67**, 034004 (2003).
[32] A. Deltuva and A. C. Fonseca, Phys. Rev. C **75**, 014005 (2007).
[33] A. Deltuva (private communication).
[34] R. Lazauskas and J. Carbonell, Phys. Rev. C **70**, 044002 (2004).

[35] E. Epelbaum, A. Nogga, W. Glöckle, H. Kamada, Ulf-G. Meissner, and H. Witala, Phys. Rev. C **66**, 064001 (2002).
[36] S. Pastore, R. Schiavilla, and J. L. Goity, Mod. Phys. Lett. A **24**, 931 (2009).
[37] A. C. Phillips, Nucl. Phys. **A107**, 209 (1968).
[38] S. F. Mughabghab, M. Divadeenam, and N. E. Holden, *Neutron Cross Sections from Neutron Resonance Parameters and Thermal Cross Sections* (Academic Press, London, 1981), http://isotopes.lbl.gov/ngdata/sig.htm.
[39] E. T. Jurney, P. J. Bendt, and J. C. Browne, Phys. Rev. C **25**, 2810 (1982).
[40] M. W. Konijnenberg, K. Abrahams, J. Kopecky, F. Stecher-Rassmussen, R. Wervelman, and J. H. Koch, Phys. Lett. **B205**, 215 (1988).
[41] M. Viviani, R. Schiavilla, and A. Kievsky, Phys. Rev. C **54**, 534 (1996).
[42] L. E. Marcucci, M. Viviani, R. Schiavilla, A. Kievsky, and S. Rosati, Phys. Rev. C **72**, 014001 (2005).
[43] S. Pastore, R. Schiavilla, and J. L. Goity, Phys. Rev. C **78**, 064002 (2008).
[44] S. Weinberg, Phys. Lett. **B251**, 288 (1990); Nucl. Phys. **B363**, 3 (1991).
[45] M. Rho, Phys. Rev. Lett. **66**, 1275 (1991).